Dear Reviewers,

Thank you for taking the time to review this manuscript. We really appreciate the reviewers' comments, which have helped us to improve the paper quality substantially. We have addressed all the comments very carefully in our following point-by-point responses. Our responses start with "R:".

The authors measured and analyzed the dust composition and microphysical features based on samples in the snowpack from a typical industrial city in China. They found that size distribution and aspect ratio of the dust did not undergo significant changes during dry and wet deposition but exhibited great variability among the different mineral composition groups. The impact of dust composition on snow albedo effect has been less studied in the past. This study using the observations to constrain dust size distribution and composition provides a useful framework to assess dust-snow albedo effect. Overall, the manuscript is well organized, but there are still some places that need more descriptions and clarifications.

Comments:

Introduction: One important missing reference here is the recent review paper (https://doi.org/10.1038/s43017-022-00379-5) on dust climatic effects, which quantifies the dust-snow radiative effects and uncertainties. This could be discussed as a broad context here for the dust-snow albedo effect problem.

R: The related reference has been added in the introduction section in Line 4-7, Page 6.

"Kok et al., (2023) also highlight that dust-snow interactions generate a global annual-mean radiative forcing of +0.013 W m^{-2} (90% confidence interval: 0.007–0.03 W m^{-2}), with large uncertainties primarily attributed to variations in dust-snow mixing state, particle size distribution, and chemical composition."

Section 2.2: (1) I would suggest presenting an example for the SEM images of the dust samples and the energy spectrum demonstrating the signals for each key dust composition elements.

R: We have added Figure S1, which shows the percentage of each elemental index (without C and O) and the corresponding SEM images of typical particles for the 12 categories of mineral particles (See Page 10, Line 7-16).

"Figure S1 presents the percentage distribution of elemental indices (excluding C and O) for 12 categories of mineral particles. Specifically, hematite-like, quartz-like, rutile-like, apatite-like, and dolomite-like particles are predominantly characterized by Fe, Si, Ti, Ca, and Mg, respectively. Kaolinite-like particles are enriched in Al and Si, while clay mineral-like and Ca-rich silicate particles contain significant amounts of Al and Si, along with notable Ca content, with the latter exhibiting a higher Ca concentration. In contrast, illite-like, smectite-like, and chlorite-like particles, in addition to being enriched in Al and Si, also contain varying amounts of K, Mg, and Fe, respectively. Correspondingly, representative SEM images of particles are presented within each mineral category panel."

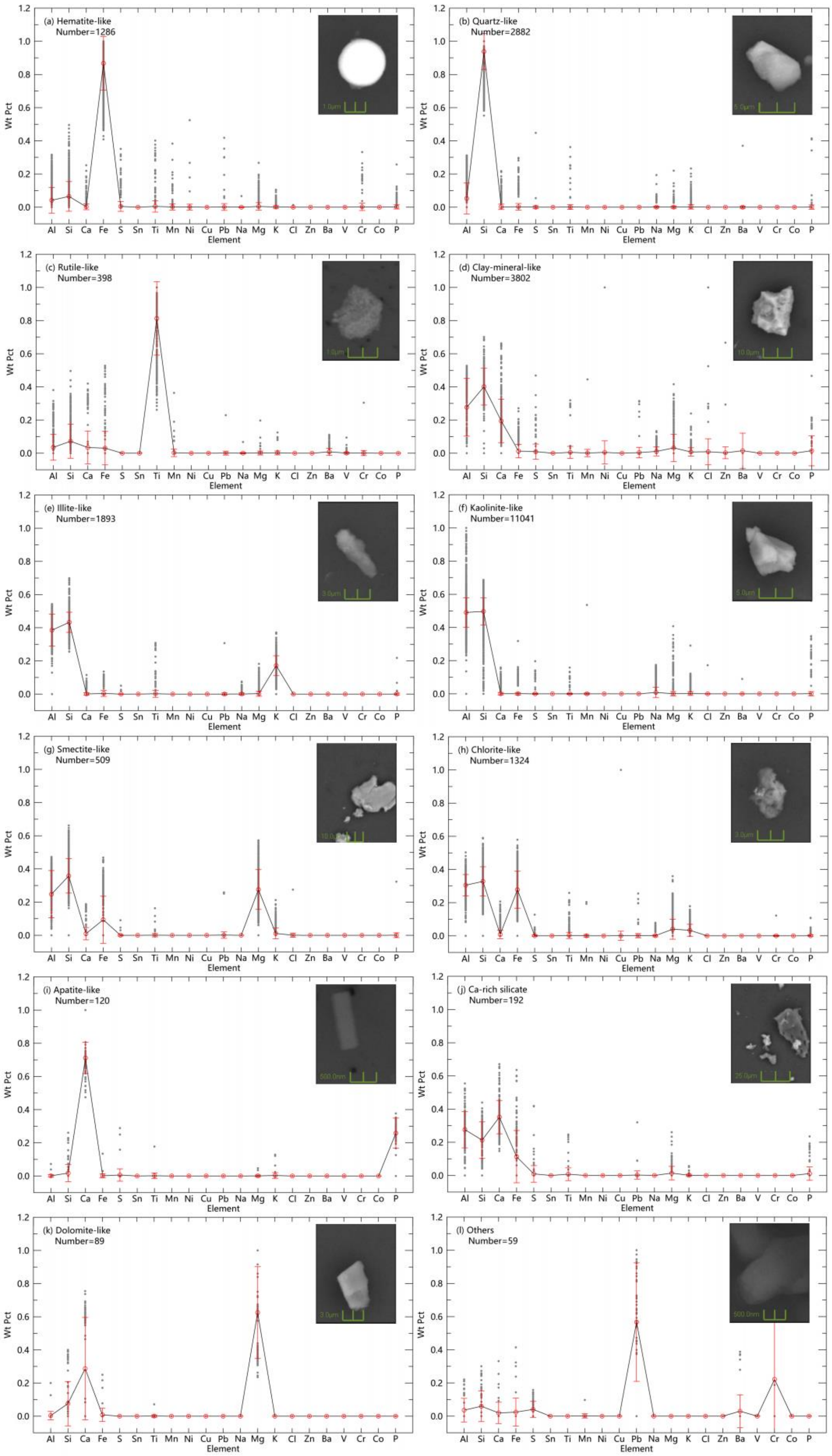

(a) Hematite-like
Number=1286
(b) Quartz-like
Number=2882
(c) Rutile-like
Number=398
(d) Clay-mineral-like
Number=3802
(e) Illite-like
Number=1893
(f) Kaolinite-like
Number=11041
(g) Smectite-like
Number=509
(h) Chlorite-like
Number=1324
(i) Apatite-like
Number=120
(j) Ca-rich silicate
Number=192
(k) Dolomite-like
Number=89
(l) Others
Number=59
Wt Pct
Element

Figure S1. The percentage of each elemental index (without C and O) for the 12 categories of mineral particles. Subplots (a)-(l) represent results for hematite-like, quartz-like, rutile-like, clay-mineral-like, illite-like, kaolinite-like, smectite-like, chlorite-like, apatite-like, Ca-rich silicates, domolite-like, and others, respectively. Correspondingly, representative SEM images of particles are presented within each mineral category panel. The red circle and whiskers denote the average value and mean deviation. The data for each particle is shown as gray solid dots.

(2) Also, it will be useful if the authors could also discuss the uncertainties associated with the SEM-EPAS measurement-analysis system.

R: We added more descriptions about the precision evaluation and potential errors in the SEM-EPAS measurement-analysis system (See Page 8, Line 10-22 and Page 9, Line 1-5).

"Compared to manually operated scanning electron microscope experiments, the IntelliSEM-EPAS^{TM} system has the advantages of intelligent control and fast analysis speed, allowing for the acquisition of a large amount of environmental particle information in a short time, including detailed data on particle concentration levels, morphology characteristics, and component content across arbitrary size ranges, and were also comparable to the results from bulk analysis (Wagner and Casuccio, 2014;Peters et al., 2016). The elemental concentrations obtained by CCSEM show good consistency with bulk analysis results from atomic absorption (AA), bulk X-ray fluorescence (XRF), proton-induced X-ray emission (PIXE), and anion chromatography (IC) (Casuccio et al., 1983). Mamane et al. (2001) also showed that 360 particles were sufficient to obtain representative results in CCSEM analysis of particle types and size distributions, based on comparisons of 360, 734, 1456, and 2819 individual particles. Although CCSEM has a superior advantage in high efficiency for measuring large quantities of particles, it encounters challenges with certain types of particles that have complex morphologies, such as soluble salts and soot (Peters et al., 2016). CCSEM-induced errors may include particle overlap, contrast artifacts, sizing inaccuracies, and particle heterogeneity (Mamane et al., 2001). Consequently, manual

error correction is typically performed prior to data processing."

(3) It is not very clear how the size distribution and aspect ratio were measured. Is it also derived from SEM images? More descriptions are needed.

R: IntelliSEM-EPAS^{TM} provides detailed measurements of the maximum and minimum diameters, average diameter, particle projection area, roundness, and aspect ratio with the acquired particle SEM images based on a built-in image processing module. Further clarification could be found in Page 8, Line 6-9.

Section 2.3: More descriptions of the SAMDS model are needed. For example, is it assuming very deep snowpack (e.g., semi-infinite)? What is the accuracy of this model? Does the model assume dust-snow external mixing as previous studies (e.g., https://doi.org/10.1029/2019MS001737) highlighted the importance of dust-snow internal mixing? How many spectral bands are used in SAMDS? Could the SAMDS handle non-spherical snow grains (I believe so)? If so, maybe a sensitivity test by using a nonspherical snow grain assumption will be very useful to quantify the uncertainty caused by snow grain shape.

R: We have added more description of SAMDS (see Page 12, Lines 5-9 and Page 13, Lines 1-5).

"The simulation of snow albedo was executed by our team's developed the Spectral Albedo Model for Dirty Snow (SAMDS) (Wang et al., 2017), which has been applied in many studies and is applicable to semi-infinite snow depth scenarios (Shi et al., 2021; Li et al., 2021). Its accuracy is also well validated, achieving an albedo accuracy of ±0.02 compared to field spectroradiometer data (Wang et al., 2017)."

"SAMDS uses 480 bands (0.2–5.0 µm) to resolve spectral albedo. Here we used $B = 1.27$ and $g = 0.89$ to characterize spherical snow grains (Wang et al., 2017), SAMDS is also capable of simulating the albedo of non-spherical snow grains, and our previous work has explored the albedo variation induced by snow grain shape (Shi et al., 2022a), which will not be reiterated here. Additionally, this study assumes dust-snow external mixing. However, it is worth noting that some studies have indicated that internal

mixing can further enhance the dust-induced albedo reduction caused by 5%–30% (He et al., 2019; Shi et al., 2021). Therefore, this assumption may underestimate the impact of dust on albedo."

Section 3.1: Based on the dust composition in this study and literature, would the authors be able to add a small discussion on potential sources for these dust particles (e.g., local or long-range transported? Anthropogenic or natural dust?)?

R: We have added more discussion on potential sources for these dust particles (see Page 15, Lines 5-10).

"Considering that industrial activities (e.g., coal combustion, urban construction, and road dust) emit quartz-rich particles, while long-range transport from arid regions (e.g., the Gobi Desert) contributes illite, which is consistent with the dust profile in Asia (Li et al., 2021). The anthropogenic contribution (e.g., hematite-like particles) aligns with the presence of nearby steel production facilities. Therefore, our results suggest that dust is likely a mixture of local and long-range sources."

Section 3.2: It is interesting to see that different mineral components show large differences in size spectra. Any physical explanation for this?

R: We have added more related physical explanations (see Page 16, Lines 13-22 and Page 17, Lines 1-3).

"Chlorite-like particles exhibited the coarsest size spectrum (median radius = 1.32 μm), nearly double that of smectite-like particles (0.57 μm), likely due to their tendency to aggregate during atmospheric transport (Formenti et al., 2014). Illite-like particles displayed the widest size range (0.38-0.59 μm) across different snow samples, possibly reflecting multiple source regions or differential atmospheric processing. The dominant kaolinite-like and quartz-like particles shared similar size distributions centered around 0.36 μm, consistent with their common origin in soil fragmentation (Kok, 2011), though kaolinite exhibited slightly less size variability. Together these components represented 51% of particles and primarily determined the overall dust size characteristics. Particularly noteworthy were hematite-like particles, which despite

being the smallest at 0.29 μm characteristic of iron oxide condensation formation, disproportionately influenced radiative properties due to their exceptional light absorption (Formenti et al., 2014; Go et al., 2022).”

Figure 4: How do these MAC_dust values compare with previous literature reported values? It will be useful to know this information. This may reflect some uniqueness of dust in this region.

R: We added detailed descriptions to compare the MAC values reported in previous literature (see Page 21, Lines 13-21).

“Overall, the measured MAC_{dust} values (0–0.3 m^2/g) show regional variations that reflect compositional differences: while comparable to Saharan dust (0.1–0.25 m^2/g, Balkanski et al., 2007), they are significantly lower than Tibetan Plateau dust (0.3–0.5 m^2/g, Li et al., 2021) and slightly higher than Colorado (San Juan Mountains) dust (0.05–0.15 m^2/g, Skiles et al., 2017). This pattern correlates with hematite content, decreasing from 8–12% in Tibetan Plateau dust to 5% in our samples and just 2–3% in Greenland dust. The distinct quartz-rich signature in our samples (15% vs <5% in other regions) may reflect unique industrial emission sources in northeastern China.”

References:

Balkanski, Y., Schulz, M., Claquin, T., and Guibert, S.: Reevaluation of Mineral aerosol radiative forcings suggests a better agreement with satellite and AERONET data, Atmos. Chem. Phys., 7, 81-95, https://doi.org/10.5194/acp-7-81-2007, 2007.

Casuccio, G. S., Janocko, P. B., Lee, R. J., Kelly, J. F., Dattner, S. L., and Mgebroff, J. S.: The Use of Computer Controlled Scanning Electron Microscopy in Environmental Studies, Journal of the Air Pollution Control Association, 33, 937-943, https://doi.org/10.1080/00022470.1983.10465674, 1983.

Formenti, P., Caquineau, S., Chevaillier, S., Klaver, A., Desboeufs, K., Rajot, J. L., Belin, S., and Briois, V.: Dominance of goethite over hematite in iron oxides of mineral dust from Western Africa: Quantitative partitioning by X-ray absorption spectroscopy, J Geophys Res-Atmos, 119, 12740-12754, https://doi.org/10.1002/2014jd021668, 2014.

Go, S. J., Lyapustin, A., Schuster, G. L., Choi, M., Ginoux, P., Chin, M. A., Kalashnikova, O., Dubovik, O., Kim, J., da Silva, A., Holben, B., and Reid, J. S.: Inferring iron-oxide species content in atmospheric mineral dust from DSCOVR EPIC observations, Atmos Chem Phys, 22, 1395-1423, https://doi.org/10.5194/acp-22-1395-2022, 2022.

He, C. L., Liou, K. N., Takano, Y., Chen, F., and Barlage, M.: Enhanced Snow Absorption and Albedo Reduction by Dust-Snow Internal Mixing: Modeling and Parameterization, J Adv Model Earth Sy, 11, 3755-3776, https://doi.org/10.1029/2019ms001737, 2019.

Kok, J. F., Storelvmo, T., Karydis, V. A., Adebiyi, A. A., Mahowald, N. M., Evan, A. T., He, C. L., and Leung, D. M.: Mineral dust aerosol impacts on global climate and climate change, Nature Reviews Earth & Environment, 4, 71-86, https://doi.org/10.1038/s43017-022-00379-5, 2023.

Li, Y., Kang, S., Zhang, X., Chen, J., Schmale, J., Li, X., Zhang, Y., Niu, H., Li, Z., Qin, X., He, X., Yang, W., Zhang, G., Wang, S., Shao, L., and Tian, L.: Black carbon and dust in the Third Pole glaciers: Revaluated concentrations, mass absorption cross-sections and contributions to glacier ablation, Sci Total Environ, 789, 147746, https://doi.org/10.1016/j.scitotenv.2021.147746, 2021.

Mamane, Y., Willis, R., and Conner, T.: Evaluation of computer-controlled scanning electron microscopy applied to an ambient urban aerosol sample, Aerosol Sci Tech, 34, 97-107, https://doi.org/10.1080/027868201300082085, 2001.

Peters, T. M., Sawvel, E. J., Willis, R., West, R. R., and Casuccio, G. S.: Performance of Passive Samplers Analyzed by Computer -Controlled Scanning Electron Microscopy to Measure PM, Environ Sci Technol, 50, 7581-7589, https://doi.org/10.1021/acs.est.6b01105, 2016.

Shi, T., Cui, J., Chen, Y., Zhou, Y., Pu, W., Xu, X., Chen, Q., Zhang, X., and Wang, X.: Enhanced light absorption and reduced snow albedo due to internally mixed mineral dust in grains of snow, Atmos Chem Phys, 21, 6035-6051, https://doi.org/10.5194/acp-21-6035-2021, 2021.

Shi, T., Cui, J., Wu, D., Xing, Y., Chen, Y., Zhou, Y., Pu, W., and Wang, X.: Snow albedo reductions induced by the internal/external mixing of black carbon and mineral dust, and different snow grain shapes across northern China, Environ Res, 208, 112670, https://doi.org/10.1016/j.envres.2021.112670, 2022.

Skiles, S. M., Painter, T., and Okin, G. S.: A method to retrieve the spectral complex refractive index and single scattering optical properties of dust deposited in mountain snow, J Glaciol, 63, 133-147, https://doi.org/10.1017/jog.2016.126, 2017.

Wagner, J., and Casuccio, G.: Spectral imaging and passive sampling to investigate particle sources in urban desert regions, Environ Sci-Proc Imp, 16, 1745-1753, https://doi.org/10.1039/c4em00123k, 2014.

Wang, X., Pu, W., Ren, Y., Zhang, X., Zhang, X., Shi, J., Jin, H., Dai, M., and Chen, Q.: Observations and model simulations of snow albedo reduction in seasonal snow due to insoluble light-absorbing particles during 2014 Chinese survey, Atmos Chem Phys, 17, 2279-2296, https://doi.org/10.5194/acp-17-2279-2017, 2017.